The Journal of Immunology

Inhalation of Toluene Diisocyanate Vapor Induces Allergic Rhinitis in Mice

Victor J. Johnson, Berran Yucesoy, Jeff S. Reynolds, Kara Fluharty, Wei Wang, Diana Richardson and Michael I. Luster

J Immunol 2007; 179:1864-1871; ;
doi: 10.4049/jimmunol.179.3.1864
http://www.jimmunol.org/content/179/3/1864

The Journal of Immunology is published twice each month by
The American Association of Immunologists, Inc.,
1451 Rockville Pike, Suite 650, Rockville, MD 20852

Print ISSN: 0022-1767 Online ISSN: 1550-6606.

Inhalation of Toluene Diisocyanate Vapor Induces Allergic Rhinitis in Mice[1]

Victor J. Johnson,[2]* Berran Yucesoy,* Jeff S. Reynolds,† Kara Fluharty,* Wei Wang,* Diana Richardson,* and Michael I. Luster*

Diisocyanates are the leading cause of occupational asthma, and epidemiological evidence suggests that occupational rhinitis is a comorbid and preceding condition in patients who develop asthma. The goal of the present studies was to develop and characterize a murine model of toluene diisocyanate (TDI)-induced rhinitis. Female C57BL/6 mice were exposed to workplace-relevant concentrations of TDI vapor via inhalation for 4 h/day for 12 days with or without a 2-wk rest period and TDI challenge. Mice exposed 12 consecutive weekdays to 50 parts per billion TDI vapor showed elevated total serum IgE and increased TDI-specific IgG titers. Breathing rates were decreased corresponding with increased inspiratory time. TDI exposure elevated IL-4, IL-5, IL-13, and IFN-γ mRNA expression in the nasal mucosa, suggesting a mixed Th1/Th2 immune response. Expressions of mRNA for proinflammatory cytokines and adhesion molecules were also up-regulated. These cytokine changes corresponded with a marked influx of inflammatory cells into the nasal mucosa, eosinophils being the predominant cell type. Removal from exposure for 2 wk resulted in reduced Ab production, cytokine mRNA expression, and cellular inflammation. Subsequent challenge with 50 parts per billion TDI vapor resulted in robust up-regulation of Ab production, cytokine gene expression, as well as eosinophilic inflammation in the nasal mucosa. There were no associated changes in the lung. The present model shows that TDI inhalation induces immune-mediated allergic rhinitis, displaying the major features observed in human disease. Future studies will use this model to define disease mechanisms and examine the temporal/dose relationship between TDI-induced rhinitis and asthma. ***The Journal of Immunology,*** **2007, 179: 1864–1871.**

Allergic rhinitis is a common inflammatory disease of the upper airways, although reported prevalence rates vary with occupation and from study to study, ranging between 5 and 65% (1). This variability may be due to varying workplace exposure and/or lack of standardized diagnostic criteria and techniques (2). It has been suggested that epidemiological studies underestimate the incidence of rhinitis in the workplace due to lack of physician awareness (3). Perhaps a more important statistic is comorbidity of occupational rhinitis in patients with occupational asthma, which has been reported to be as high as 92% (4). This same study indicated that development of rhinitis symptoms often precedes the appearance of asthma symptoms by up to 1 year. In addition, a recent study investigating the economic impact of occupational diseases claimed that allergic rhinitis is the most costly disease in terms of absenteeism and lost work productivity. On average, workers with rhinitis were absent 3.6 days per year and unproductive for 2.3 h per workday when symptomatic. Cost estimates indicate $593/year in productivity losses per employee with rhinitis vs $85/year for employees with asthma (5).

Mechanistic investigations of occupational allergic airway diseases have focused primarily on asthma, with few studies directed toward understanding the pathogenesis of rhinitis, especially for disease caused by low m.w. chemicals. Asthma studies in humans exposed to diisocyanates and animal models suggest that T lymphocytes are critical to disease and orchestrate a mixed Th1/Th2 immune response (6). Diisocyanate-specific T cell clones, Th2 cytokines, including IL-4 and IL-5, as well as Th1 cytokines, such as IFN-γ, have been identified in the respiratory mucosa of workers following exposure to diisocyanates (7–9). Important roles for Th2 and Th1 cytokines, as well as specific Abs, have been confirmed using transgenic approaches in animal models of diisocyanate asthma (10, 11). According to the united airways disease and one airway-one disease hypotheses, the upper and lower respiratory tract are likely to share common fundamental susceptibilities to allergic responses (12, 13). Therefore, many of the disease mechanisms responsible for diisocyanate-induced asthma are expected to also play a role in rhinitis, although few studies have been conducted to support this conclusion. Occupational studies support the development of challenge-responsive rhinitis in exposed workers as well as an association with diisocyanate-specific Abs (14–16).

Workplace exposure to diisocyanates is complex and varied, the nature of which is dependent upon the compounds being used. Exposure to the highly volatile toluene diisocyanate (TDI)[3] can occur as vapor, aerosol, or a mixture of both, whereas less volatile polyisocyanates are usually present as aerosols. Nevertheless, respiratory sensitization and symptoms have been associated with

*Toxicology and Molecular Biology Branch and †Pathology and Physiology Research Branch, Health Effects Laboratory Division, National Institute for Occupational Safety and Health, Centers for Disease Control and Prevention, Morgantown, WV 26505

Received for publication Febuary 15, 2007. Accepted for publication May 23, 2007.

The costs of publication of this article were defrayed in part by the payment of page charges. This article must therefore be hereby marked *advertisement* in accordance with 18 U.S.C. Section 1734 solely to indicate this fact.

[1] These studies were funded in part by a National Institute of Environmental Health Services-National Institute for Occupational Safety and Health Interagency Agreement (Y1-ES-0001, Immunotoxicity of Workplace Xenobiotics). The findings and conclusions in this report are those of the authors and do not necessarily represent the views of the National Institute for Occupational Safety and Health.

[2] Address correspondence and reprint requests to Dr. Victor J. Johnson, Toxicology and Molecular Biology Branch, Health Effects Laboratory Division, National Institute for Occupational Safety and Health, 1095 Willowdale Road, Mail Stop 3014, Morgantown, WV 26505-2888. E-mail address: vjohnson3@cdc.gov

[3] Abbreviations used in this paper: TDI, toluene diisocyanate; MRM, magnetic resonance microscopy; PAS, periodic acid-Schiff; ppb, parts per billion; RIS, remote intelligent sensor; PenH, enhanced pause.

exposure concentrations at or above 5–10 parts per billion (ppb) (17), and asthmatic reactions have been induced following exposure to as low as 1 ppb TDI in previously sensitized individuals (18). In addition, workers with skin staining were more likely to develop respiratory symptoms, implicating dermal exposure as a potential route of sensitization in human (19). These studies illustrate the complexity of the exposure-response relationship for diisocyanates. Several murine models have been developed to investigate the etiopathogenesis of occupational asthma induced by diisocyanates and have been reviewed by Johnson and Luster (6). Routes of sensitization and challenge are varied between models and include s.c. and epicutaneous skin exposure, intranasal installation, aerosol inhalation, and vapor inhalation. In contrast, few studies have focused on the effects of diisocyanates in the upper respiratory tract, and direct comparisons of upper and lower airway effects are lacking. Our laboratory has previously demonstrated that inhalation of TDI vapor leads to inflammation in the nose and lung (allergic rhinitis and asthma, respectively), although extensive exposure-response relationships were not defined (20, 21).

A paucity of research is available regarding the etiology of occupational rhinitis and the relationship between occupational rhinitis and asthma. The goal of the present study was to develop and characterize a murine model of occupational rhinitis induced by inhalation exposure to TDI vapor, a workplace-relevant exposure route. This model should prove useful in examining mechanisms and identifying biomarkers useful for early diagnosis, treatment, and prevention of occupational allergic respiratory disease.

Materials and Methods

Exposure system

TDI (Mondur TD80 grade A; 80 and 20% mixture of 2,4- and 2,6-isomers, respectively) was provided by Bayer, Polyurethanes Division. The exposure chamber was a 1200 L stainless steel live-in chamber (Unifab) supplied with high efficiency particulate air filter-purified and conditioned air providing eight air changes per hour and maintaining temperature and humidity at 23 ± 2°C and 50 ± 5%, respectively. Temperature was controlled by facility heating, ventilating, and air conditioning system, and the humidity was controlled by passing the dilution air supply over the surface of a variable temperature in-line water bath. A similar chamber setup was used for the sham air exposure. Mice were housed in hanging stainless steel mesh cages, remained in the chambers continuously from Monday morning through Friday afternoon, and were returned to microisolator cages over the weekend. A custom Labview (v7.0; National Instruments) application was designed to control and monitor set points for temperature (21–25°C; HMP243; Vaisala), humidity (40–60%; HMP243; Vaisala), pressure (−1.5 cm H_2O; model 264; Setra Systems), and TDI concentration (50 ± 5 ppb; RIS TDI analyzers; Scott Safety and Health) based on feedback from sensors mounted in the chambers. Generation of a TDI vapor atmosphere that was free of TDI aerosol was achieved by passing dried high efficiency particulate air filter-filtered air over a 50-cm^2 surface of liquid TDI. Chamber TDI concentrations were regulated by adjusting air flow through the TDI generator. The TDI vapor entered a mixing chamber and was diluted with a fixed flow of dilution air before entering the exposure chamber. Air flows were controlled by computer-interfaced mass flow controllers (Aalborg Instruments), and TDI concentrations were monitored in real time using RIS TDI analyzers (Scott Safety and Health) located in two locations within the chamber. The RIS units were calibrated using a fluorescamine assay with a detection limit of 10 ng/ml, as previously described, with modifications (22). Chamber air samples (1 L/min for 15 min) were collected using impingers containing 10 ml of 0.5% H_2SO_4, and then a 0.5-ml sample was added to 0.5 ml of saturate sodium tetraborate, followed by addition of 0.05 ml of fluorescamine (1.5 mg/ml in acetonitrile) while vortexing. Fluorescence was read on an LS-50B spectrofluorometer (PerkinElmer) with 410 nm excitation and 510 nm emission wavelengths. Exposure chambers were maintained at negative pressure (−1.5 cm H_2O) to prevent TDI leaks into the inhalation facility. Exhaust air was filtered through activated charcoal and tested for residual TDI before entering the building exhaust. Food and water were removed during the TDI exposure to prevent contamination.

Experimental animals

Female inbred C57BL/6 mice were purchased from The Jackson Laboratory at 5–6 wk of age. Upon arrival, the mice were quarantined for 2 wk and acclimated to a 12-h light/dark cycle. Animals were housed in ventilated microisolator cages in environmentally controlled conditions at National Institute for Occupational Safety and Health animal facilities in compliance with American Association for the Accreditation of Laboratory Animal Care-approved guidelines and an approved Institutional Animal Care and Use Committee protocol. The animal rooms are monitored for specific pathogens through disease surveillance and a sentinel animal program. Food and water were provided ad libitum. Mice were randomized among three treatment protocols, as follows: 1) sensitization: 12 consecutive weekday exposures to 50 ppb TDI for 4 h/exposure with mice euthanized 24 h after final exposure (sensitized group); 2) recovery: exposed as in group 1, but allowed to rest for 2 wk before examination (recovery group); and 3) challenge: exposed as in group 2, followed by 3 consecutive days of exposure at 50 ppb TDI for 4 h/exposure with euthanasia 24 h following final exposure (challenged group). The two control groups included mice exposed to air during sensitization (control) and air-exposed mice challenged with 50 ppb TDI for 4 h/day for 3 consecutive days (challenge only).

Tissue collection and histology

Two groups of mice were used for each exposure protocol, one for mRNA analysis and the other for pathology. Mice were sacrificed via CO_2 inhalation 24 h following the final exposure. Blood was collected from the abdominal aorta, and serum was isolated and frozen at −80°C. Magnetic resonance microscopy (MRM) was used to show the anatomic locations of tissues used for analysis of mRNA expression in relation to the planes of section used for pathology assessment (see Fig. 1). MRM imaging of contrast enhanced (10% Prohance perfusion; Bracco Diagnostics), formalin-fixed mouse heads was performed by MRPath using a 7 Tesla magnet (Magnex Scientific Products). Proton density images were acquired at 48 μm isotropic resolution, and the turbinates were color coded using Photoshop software. For mRNA analysis, the head was removed and the nasal cavity was flushed with RNAlater; the top of the skull, the brain, and the lower jaw were removed, and the remaining tissue was stored in 10 vol of RNAlater at 4°C until regional dissection. The lungs were inflated with RNAlater and stored at −20°C. The nasal cavity was opened by removing the nasal bones and flattening the skull along the anterior-posterior axis. Using blunt dissection, the nasal mucosa was divided into four regions, as follows: the nasoturbinates, maxilloturbinates/lateral wall, septum, and ethmoturbinates. Fig. 1 shows the tissue areas that constitute each region. All dissections for gene expression analysis were performed with the head immersed in RNAlater to prevent mRNA degradation.

For pathology, lungs were inflated and the nasal cavity was filled via a tracheal cannula with 10% neutral buffered formalin. The trachea was then ligated to maintain the lungs inflated, and the head and lungs were immersed in 10% neutral buffered formalin for 18 h. The nose was decalcified in Immunocal (Decal Chemical) for 7 days, followed by gross dissection into four sections (T1–T4), according to previously established guidelines (23). The anatomical locations of sections T1–T4 are shown in Fig. 1. The nasoturbinates, maxilloturbinates, and lateral wall are visible in sections T1 and T2; the ethmoturbinates in sections T3 and T4; and the septum extends the length of the nasal cavity. Fixed tissues were embedded in paraffin, sectioned at 5 μM, and stained with H&E for histopathological assessment. Periodic acid-Schiff (PAS) staining was performed to identify goblet metaplasia and Hansel's staining for eosinophil identification. Morphometry was performed using digital photomicrographs acquired using a Retiga 2000R digital camera (QImaging) attached to an Olympus AX70 photomicroscope (Olympus America). Images were captured using SimplePCI (Compix; Imaging Systems) and analyzed using Optimas 6.5 Image analysis software (Media Cybernetics) by counting the number of eosinophils/mm basement membrane (all cells between the epithelial surface and the bone were counted). A minimum of five high-power fields was counted per structure for each mouse. Mucosal thickness was measured by drawing tangents from the epithelial surface to the interface between the bone and lamina propria. A minimum of 10 tangents was measured per structure for each mouse.

Assessment of airway function

Respiratory function was assessed immediately following the final TDI sensitization exposure using unrestrained whole body plethysmography (Buxco Electronics), as previously described (20, 24). Mice were placed into individual plethysmographs and allowed to acclimate for 10 min. Baseline breathing parameters were collected for 15 min.

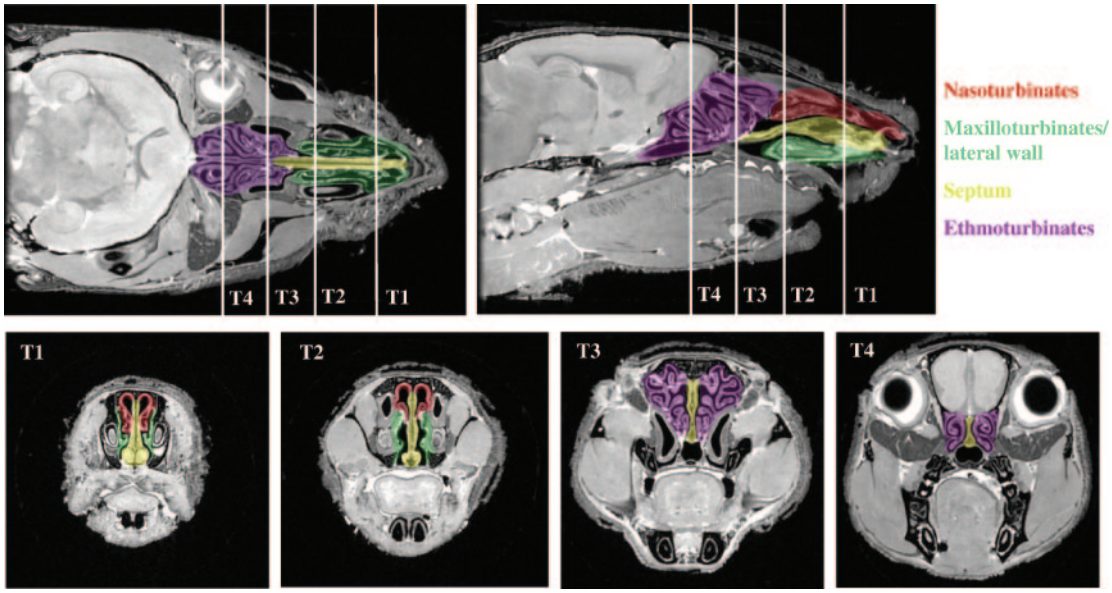

FIGURE 1. MRM of the murine head. MRM images of a representative mouse head were color coded to display the locations of tissues collected for gene expression analysis, with red, green, yellow, and purple shading representing the nasoturbinates, maxilloturbinates, septum, and ethmoturbinates, respectively. Views of the entire mouse head are shown in the frontal plane of section (*upper left panel*), sagittal plane of section (*upper right panel*), and transverse plane of section (*lower four panels*). The vertical white lines on the *upper panels* represent the transverse planes examined for pathology, with the label, T1–T4, being on the anterior face of the four tissue blocks. Anatomy of the transverse plane at each pathology level is shown in the *lower panels*.

TDI-specific IgG and total serum IgE detection

TDI-specific IgG serum Abs were detected using an ELISA procedure, as previously described (20, 24), with modifications where noted. The TDI-mouse serum albumin conjugate used as the capture Ag was prepared by adding 0.5 ml of dilute TDI (1% in acetone) to 10 ml of mouse serum albumin (5 mg/ml in PBS) using a KDS100 syringe pump (KD Scientific) at 25 μl/min. The resulting conjugate solution was centrifuged at 10,000 $\times$ *g* for 1 min, followed by extensive dialysis against PBS. The purified conjugate was filtered through a 0.2-μm membrane, aliquoted, and stored at -80°C. A cutoff OD at 650 nm (OD_{650}) of 0.1 (average OD_{650} of challenge-only mouse serum was 0.06 $\pm$ 0.005) was used to determine the titer by extrapolation from log-log curve fits (dilution vs absorbance) generated for each sample using a custom Matlab (v6.5; The MathWorks) application. Total serum IgE was determined using BD OptEIA mouse IgE ELISA (BD Pharmingen) as per the manufacturer's instructions.

Real-time RT-PCR assessment of nasal mucosa gene expression

Tissues were homogenized, and total cellular RNA was extracted using the Qiagen RNeasy kit (Qiagen), according to the manufacturer's instructions. RNA (1 μg) was reverse transcribed using random hexamers and 60 U of Superscript II (Invitrogen Life Technologies). Real-time PCR primer/probe sets for murine IL-1β, IL-4, IL-5, IL-13, IFN-γ, TNF-α, and 18S were purchased from Applied Biosystems. Primers for ICAM-1 (forward, GAGTTTTACCAGCTATTTATTGAGTACCC; reverse, CTCTCACAG CATCTGCAGCAG) and VCAM-1 (forward, TTAAAGTCTGTGGATG GCTCGTAC; reverse, CTTAATTGTCAGCCAACTTCAGTCTT) were

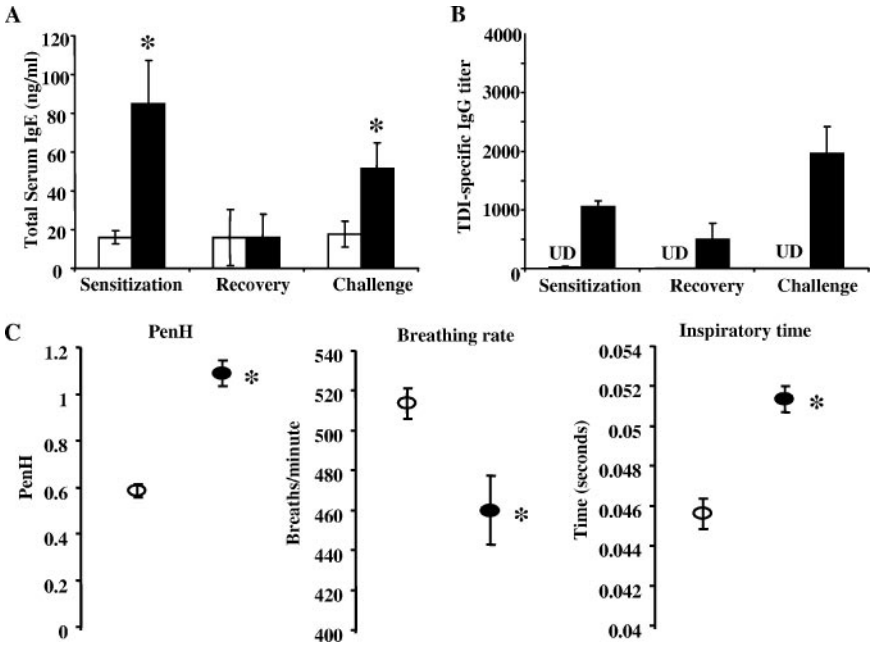

FIGURE 2. Effect of TDI inhalation exposure on serum Ab production and breathing pattern in mice following TDI sensitization, recovery, and challenge. Mice were exposed to 50 ppb TDI vapor for 4 h/day for 12 consecutive weekdays with or without a 2-wk rest period and subsequent inhalation challenge. *A*, Total serum IgE was determined using a commercial ELISA kit. *B*, Serum titers of TDI-specific IgG Abs were determined using a custom ELISA, as outlined in *Materials and Methods*. Mice were euthanized and blood samples were taken 24 h following the twelfth exposure for the sensitization protocol, after resting for 2 wk subsequent to exposure for the recovery protocol and 24 h following the third inhalation challenge for the challenge protocol. □, Control group; ■, mice treated with TDI. *C*, Breathing parameters including PenH, breathing rate, and inspiratory time were measured using whole body plethysmography immediately following the twelfth sensitization exposure to TDI. ○, Control mice; ●, mice treated with TDI. UD, undetected; mean $\pm$ SEM ($n = 5$); $*$, significantly different from respective control group at $p < 0.05$.

designed for SYBR green analysis using Primer Express software (Applied Biosystems). Real-time PCR was performed using Taqman or SYBR Green Universal Master mix with amperase in an Applied Biosystems 7900HT (Applied Biosystems) for 1 cycle at 50°C for 2 min (degrade carryover using amperase) and 95°C for 10 min, followed by 60 cycles at 95°C for 15 s and 60°C for 1 min. Relative differences in mRNA expression between control and treatment groups were determined by the relative quantification method developed by Pfaffl (25). This method uses gene-specific PCR efficiencies to more accurately generate relative changes based on threshold cycle. Target gene expression was normalized to the housekeeping gene 18S/rRNA.

Statistical analysis

Studies were conducted using a randomized complete block design. Due to unequal variances between treatment groups, the analyses were performed using the raw data and log-transformed data (equalized variances in all cases). No substantive differences between the two analyses were found, and thus the empirical data are presented in all figures. Treatment effects were determined using one-way ANOVA, followed by Fisher probable least squares difference posthoc test (26). Student's *t* test was used when the experimental design consisted of two groups. Treatment effects on TDI-specific Ab titers were analyzed using the Wilcoxon rank sum test. Differences were considered significant at $p < 0.05$. All experiments were replicated, and representative data are shown.

Results

Breathing TDI vapor increases total serum IgE and TDI-specific IgG Abs

TDI inhalation increased total serum IgE following sensitization or challenge (Fig. 2*A*). Ag-specific IgE was not detected in the current model of inhalation exposure to TDI vapor (data not shown), as is common to many murine models of occupational airways disease. This may be due to low TDI-specific IgE production and/or poor assay sensitivity (27), although TDI-specific IgE Abs have been detected following a very rigorous s.c. sensitization protocol (21). Total serum IgE returned to control levels after a 2-wk rest period with no TDI exposure (Fig. 2*A*). All mice treated with TDI vapor produced high titers of TDI-specific IgG Abs (Fig. 2*B*). TDI-specific IgG Ab titers also decreased 2 wk after the last sensitization exposure (Fig. 2*B*). Challenge of sensitized mice with TDI vapor significantly increased the serum titer of TDI-specific IgG Abs, with levels exceeding those observed immediately following the sensitization protocol (Fig. 2*B*). Total serum IgE levels were also increased following challenge of sensitized mice (Fig. 2*A*). It should be noted that TDI challenge did not influence the level of IgE (Fig. 2*A*) or TDI-specific IgG (Fig. 2*B*) in naive mice.

These Ab responses were accompanied by changes in breathing pattern manifested as a doubling in baseline enhanced pause (PenH) (Fig. 2*C*). Exposed mice showed decreases in respiratory rates that corresponded with increases in inspiratory time.

Inhalation exposure to TDI vapor resulted in extensive allergic inflammation of the nasal mucosa

The anatomical locations of the transverse planes, T1–T4, that were examined for pathological changes are shown in Fig. 1. Representative histopathological changes in the nasal mucosa associated with sensitization to TDI vapor are shown in Fig. 3. Inhalation of TDI vapor caused extensive inflammatory cell infiltration into the lamina propria underlying the transitional and respiratory epithelium of the nasal mucosa (Fig. 3, *C* and *D*). The inflammatory infiltrates consisted predominantly of eosinophils (cells with red-orange cytoplasm in Fig. 3*E*), although lymphocytes (open arrowheads in Fig. 3*E*) and plasma cells (filled arrows in Fig. 3*E*) were readily apparent. The identity of the eosinophils was confirmed using Hansel's stain, evidenced by the brilliant red-orange cytoplasm due to uptake of eosin specifically by eosinophil granules (Fig. 3*F*). These cells also had a bilobed nucleus, another distinguishing feature of eosinophils. Minimal, but significant influx of eosinophils was evident in the nasal mucosa of the maxilloturbinates and nasoturbinates of naive mice as early as 24 h following the third challenge exposure (challenge-only group, 18 ± 7 eosinophils/mm basement membrane; Fig. 4*A*). Eosinophil infiltration

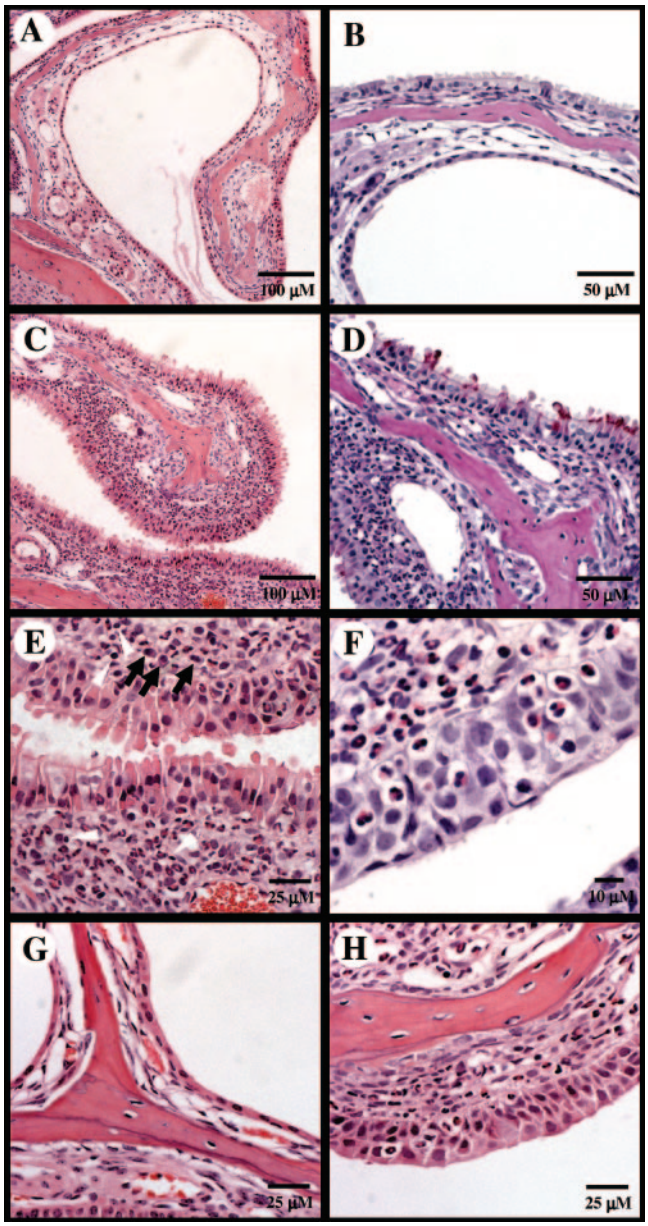

FIGURE 3. Histopathology in the nasal mucosa following TDI inhalation in mice. Mice were euthanized 24 h following the twelfth exposure to air (control group) or TDI and prepared for pathological analysis, as detailed in *Materials and Methods*. *A*, H&E section of the maxilloturbinate and lateral wall from a control mouse; PAS-stained section of the maxilloturbinate from a control mouse (*B*); H&E section of the maxilloturbinate and lateral wall from a TDI-exposed mouse (*C*); PAS-stained section of the maxilloturbinate from a mouse exposed to TDI vapor (*D*); H&E section showing the epithelium of the maxilloturbinate and lateral wall of a TDI-exposed mouse (filled arrows and open arrowheads identify plasma cells and lymphocytes, respectively) (*E*); Hansel's stained section of the maxilloturbinate of a TDI-exposed mouse identifying eosinophil infiltration into the lamina propria and epithelium (*F*); H&E section of transitional epithelium from a control mouse (*G*); H&E section of transitional epithelium from a TDI-exposed mouse showing thickened epithelium due to epithelial cell hypertrophy (*H*). The photomicrographs are representative of five mice per group.

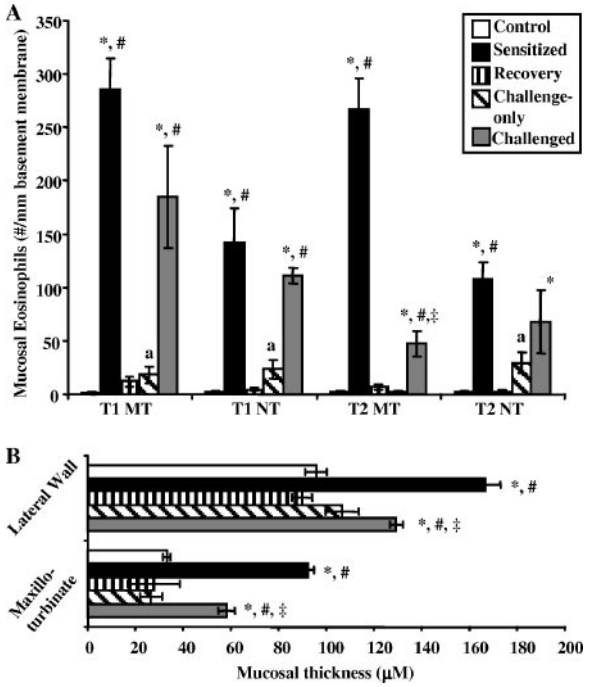

FIGURE 4. Morphometric analysis of TDI-induced inflammation in the nasal cavity of mice. Mice were treated for 4 h/day for 12 consecutive weekdays with 50 ppb TDI vapor and represent the sensitized group. The recovery group was rested for 14 day after sensitization exposure, and the challenged groups were re-exposed to 50 ppb TDI 4 h/day for 3 days. Control mice were exposed to filtered air during the sensitization protocol, and challenge-only mice were treated with filtered air during the sensitization protocol, rested for 2 wk, and then challenged with 50 ppb TDI 4 h/day for 3 days. Mice were euthanized and tissue was prepared for pathology 24 h following the twelfth exposure for the control and sensitized groups, after resting for 2 wk subsequent to exposure for the recovery group and 24 h following the third inhalation challenge for the challenge-only and challenged groups. Measurements were captured from calibrated digital images, according to *Materials and Methods*. *A*, Quantification of eosinophil infiltration per unit length (mm) of basement membrane at levels T1 and T2. *B*, Measurement of mucosal thickness of the maxilloturbinate and lateral wall of the nasal cavity at the level of T2. MT, Maxilloturbinate; NT, nasoturbinate. Mean ± SEM ($n = 5$); significantly different from ∗, control; #, challenge only; and ‡, sensitized; a, significantly different from control group using Student's *t* test.

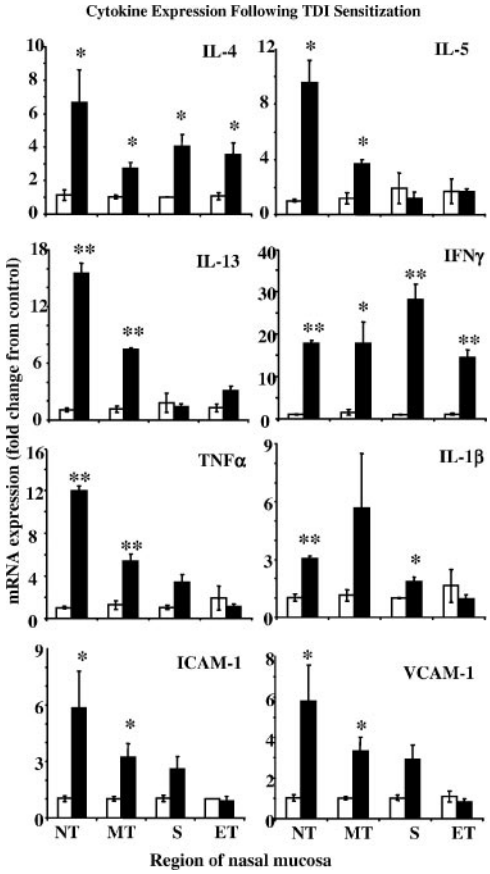

FIGURE 5. Effect of TDI inhalation on the expression of immune and inflammatory cytokines and adhesion molecules in the nasal mucosa of mice. Mice were treated 4 h/day for 12 consecutive weekdays with 50 ppb TDI vapor and subsequently euthanized 24 h following the last exposure. Nasal tissue was preserved in RNAlater and dissected into regions (see Fig. 1), and gene expressions for IL-4, IL-5, IL-13, IFN-γ, TNF-α, IL-1β, ICAM-1, and VCAM-1 were determined using real-time PCR. Data are expressed as fold change in mRNA expression in the TDI-exposed mice relative to air control mice. □, Control; ■, sensitized; NT, nasoturbinate; MT, maxilloturbinate; S, septum; ET, ethmoturbinate. Mean ± SEM ($n = 5$). Significantly different from respective control group within the specific nasal regions at ∗, $p < 0.05$; ∗∗, $p < 0.01$.

increased markedly in the sensitized group to 276 ± 29 eosinophils/mm basement membrane (control mice showed ~2 ± 1 eosinophil/mm). This inflammatory response was also manifested as thickening of the mucosa lining the lateral wall of the nasal cavity and the maxilloturbinate by 175 and 275%, respectively, in sensitized mice relative to the control group (Fig. 4*B*). Discontinuing exposure for 2 wk resulted in reduction in cellular inflammation to control levels. Rested mice were then challenged with three consecutive exposures for 4 h/day at 50 ppb TDI, and the same pathological parameters were examined. Challenge resulted in eosinophil influx (Fig. 4*A*) and mucosal thickening (Fig. 4*B*) in previously sensitized mice, whereas only minimal, but significant, eosinophil influx was observed in the challenge-only group (Fig. 4*A*). The pathology described above characterizes the response in the nasoturbinates and maxilloturbinates, whereas negligible inflammation was evident in the septum or the ethmoturbinate regions of the nasal cavity (data not shown). In addition to cellular inflammation, changes in the nasal epithelium were observed in mice immediately following the TDI sensitization protocol. Goblet metaplasia in the epithelium lining the maxilloturbinate was evident by the characteristic purple staining of mucus proteins with PAS (Fig. 3*D*). Hyalinosis was also observed in the transitional epithelium of the maxilloturbinate and lateral wall, with many cells excreting hyaline eosinophilic globules into the lumen of the nasal cavity (Fig. 3, *C* and *E*). TDI-exposed mice also showed hyperplasia of the transitional epithelium lining the lateral wall and turbinates in the anterior region of the nose (Fig. 3*H*). This epithelium is normally a single cell layer covering the lamina propria, as observed in the control group (Fig. 3, *A*, *B*, and *G*) and the challenge-only group (data not shown), but increased to three to four cells thick following exposure to TDI vapor. In addition, numerous eosinophils were seen invading the altered epithelium in TDI-exposed mice (Fig. 3, *E*, *F*, and *H*). The current exposure parameters did not induce inflammation in the lung despite the dramatic inflammation observed in the nose (data not shown).

Cytokine expression in the nasal mucosa indicates a mixed Th1/Th2 response

Real-time PCR was used to determine the expression of key immune and inflammatory genes in the nasal mucosa following regional dissection. Fig. 1 shows the anatomical locations of the

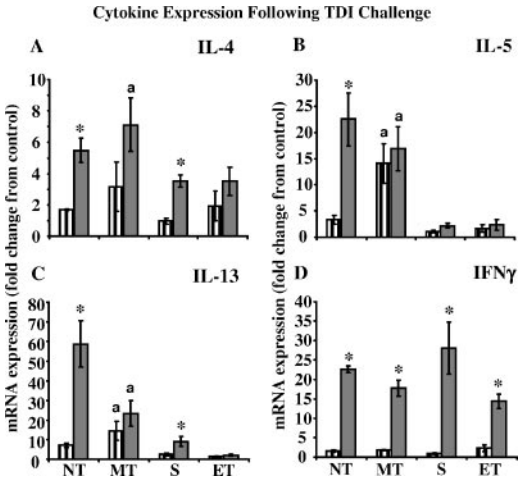

FIGURE 6. Effect of TDI challenge on the expression of Th1/Th2 cytokines in the nasal mucosa of mice. Mice were sensitized for 4 h/day for 12 consecutive weekdays with 50 ppb TDI vapor and subsequently allowed to recover for 2 wk. Mice were challenged for 4 h/day on 3 consecutive days with 50 ppb TDI and euthanized 24 h following the third challenge. Nasal tissue was preserved in RNAlater and dissected into regions according to Fig. 1, followed by real-time PCR analysis of gene expression for IL-4, IL-5, IL-13, and IFN-γ. Data are expressed as fold change in mRNA expression in the challenge-only group (▥) or the challenged group (▨) relative to control mice. *A*, Nasoturbinate (NT); *B*, maxilloturbinate (MT); *C*, septum (S); *D*, ethmoturbinate (ET). Mean ± SEM ($n = 5$). Significantly different from ∗, control and challenge-only groups or a, control group at $p < 0.05$.

tissues used for gene expression analysis. TDI-induced changes in the expression of Th2 cytokines IL-4, IL-5, and IL-13 and the Th1 cytokine IFN-γ in the nasoturbinates, maxilloturbinates, septum, and ethmoturbinates are shown in Fig. 5. The expressions of all cytokines examined were induced significantly in the nasoturbinate following sensitization with TDI. Elevated expression of all four cytokines was also observed in the maxilloturbinate, although the induction was approximately half of that observed in the nasoturbinate. Fewer changes in gene expression were observed in the septum and ethmoturbinates, although IL-4 and particularly IFN-γ were induced in these regions.

We also examined the expression of inflammatory cytokines and adhesion molecules that are known to be integral to the local recruitment of inflammatory effector cells. The regional mRNA expressions of TNF-α, IL-1β, ICAM-1, and VCAM-1 following sensitization with TDI are shown in Fig. 5. Strong induction of TNF-α was observed in the nasoturbinates and maxilloturbinates, with the intensity of changes similar to that observed for the Th1/Th2 cytokines. Expression of IL-1β also increased in these regions, but to a lesser extent. ICAM-1 and VCAM-1 were up-regulated in the nasoturbinates and maxilloturbinates, and most likely play an important role in adhesion and extravasation of the eosinophils and lymphocytes into the lamina propria and epithelium of the nasal mucosa. The current exposure paradigm did not alter cytokine expression in the lung, a finding that corresponds with the lack of pathological changes in the lung (data not shown).

Re-exposure to TDI vapor induces rapid cytokine expression in the nasal mucosa of sensitized mice

Gene expression in the nasal mucosa returned to control levels subsequent to removal from exposure for 2 wk (data not shown). Inhalation challenge with TDI resulted in robust up-regulation of both Th1 and Th2 cytokines (Fig. 6). The expressions of IL-4, IL-5, IL-13, and IFN-γ were induced in the nasoturbinates (Fig. 6*A*) and maxilloturbinates (Fig. 6*B*), whereas IL-4, IL-13, and IFN-γ were induced in the septum (Fig. 6*C*) and only IFN-γ was induced in the ethmoturbinates (Fig. 6*D*) of sensitized mice subsequent to challenge. The expression of Th2 cytokines was greatest in the anterior regions of the nose (nasoturbinates and maxilloturbinates), whereas the up-regulation of IFN-γ was consistent across all regions from the anterior to posterior aspects of the nasal mucosa. The expression of IL-13 was increased in the nasoturbinates and maxilloturbinates of challenge-only mice relative to the control group (Fig. 6, *A* and *B*), which is consistent with the mild accumulation of eosinophils in the nasoturbinates and maxilloturbinates after challenge in this group (Fig. 4*A*).

Discussion

Symptoms of occupational rhinitis include sneezing, itching, rhinorrhea, and nasal obstruction, and, in this respect, are similar to allergic rhinitis caused by environmental Ags. The underlying mechanisms driving occupational rhinitis also appear to share similarities with allergic rhinitis caused by ubiquitous airborne protein allergens, although these mechanisms are only beginning to be understood and, in some cases, may involve nonallergic pathways. For example, high and low m.w. occupational asthmogens can cause sensitization through classical IgE-mediated pathways, whereas evidence supports additional non-IgE mechanisms for disease caused by low m.w. chemicals (3). The inflammatory response in the nasal mucosa of allergic rhinitis patients is dominated by eosinophils and lymphocytes with T cell cytokines, including IL-4, IL-5, and IL-13 being important (28), although the role of such mediators in the pathology of TDI-induced occupational rhinitis remains unknown. In the present study, mice treated with TDI vapor showed extensive inflammation of the nasal mucosa, with eosinophils being the predominant cell type. The inflammation was associated with a mixed Th1/Th2 immune response similar to diisocyanate asthma. Mucosal inflammation corresponded with changes in breathing parameters as well as increased IgE and TDI-specific IgG Abs in the serum. Collectively, our model displays many key features characteristic of allergic rhinitis in humans. The inflammation and gene expression changes were isolated to the upper airways, because the lower airways showed no evidence of inflammation. This suggests that the changes observed in the nasal mucosa were most likely due to local Ag recognition, processing, and presentation to effector cells at the site of exposure.

Eosinophils are a prominent inflammatory cell present in the nasal mucosa of patients with active allergic rhinitis and were, by far, the most predominant cell type in our TDI model. These cells store numerous toxic granule proteins (eosinophil peroxidase, eosinophil cationic protein, and major basic protein), lipid mediators (leukotrienes and platelet-activating factor), and other products with immunomodulatory properties. Activation results in the release of these mediators into the tissues and probably constitutes a substantial contribution to the physiological and pathological changes evident in rhinitis. In fact, several studies show that eosinophils and their mediators display the highest correlation with symptomology, nasal airflow, pulmonary function, and nasal pathology in allergic rhinitis patients (29, 30). The present model demonstrates extensive eosinophil infiltration, resulting in thickening of the lamina propria of the anterior turbinates and lateral wall. These changes are likely to contribute to narrowing of the lumen and nasal airflow obstruction. Analysis of breathing patterns showed increased PenH and decreased breathing rate, two parameters that correlate with direct measures of nasal obstruction in

rhinitic mice (31). Although the absolute changes in breathing parameters were small, they are typical of Ag-driven responses in allergic mice (32, 33). Eosinophils were also noted invading the epithelium that lines the nasal mucosa, and activation and release of toxic mediators from these cells may be responsible for some of the epithelial hyperplasia/metaplasia, hyalinosis, and damage.

The cytokine fingerprint induced by inhalation exposure to TDI is indicative of allergic rhinitis and correlates with the substantial influx of eosinophils. TNF-α and IL-1β are increased, the source of which may be dendritic cells or activated mast cells. These proinflammatory cytokines have been shown to induce the production of adhesion molecules (34, 35) as well as eosinophil and lymphocyte chemotactic factors in the nasal mucosa of allergic rhinitis patients (36, 37). This response can be amplified by Ag-specific activation of T lymphocytes, another constituent of the inflammation in the present model. We observed increase expression of IL-4, IL-5, and IL-13 in the nasal mucosa of mice exposed to TDI vapor. IL-4 and IL-13 can act in concert with proinflammatory cytokines to stimulate epithelial cells, effectively boosting the production of chemokines that recruit eosinophils (38), and have been shown to act synergistically with TNF-α to induce thymus- and activation-regulated chemokine, an important T lymphocyte chemokine, in the nasal mucosa (36). In addition, IL-5 is key to the survival and priming of eosinophils, leading to heightened activation of effector functions (39). Although respiratory allergy is largely thought of as a Th2-mediated disease, substantial evidence supports an important role for Th1 responses. For example, cooperation between Th1 and Th2 cells is important for a robust eosinophil response in OVA asthma (40). In this respect, IFN-γ was markedly increased in the mucosa of mice following sensitization and also after challenge in the present model, suggesting that Th1 responses are important in TDI rhinitis, a finding consistent with human studies of TDI asthma (41, 42). IFN-γ is known to promote Th2-mediated allergic inflammation and can also amplify the effects of proinflammatory cytokines on chemokine up-regulation in nasal epithelial cells (37). This cumulative evidence suggests the possibility that lymphocytes and eosinophils (and other immune cells) establish a feedback signaling network that culminates in the pathophysiology observed in TDI-treated mice.

It should be noted that IL-13 expression was significantly up-regulated in naive mice following 3 days of challenge (challenge-only group) with TDI vapor. IL-13 expression was increased only in the nasoturbinates and maxilloturbinates and not in the mucosa of the posterior nasal cavity. This finding indicates that TDI acts as a strong hapten and exposure to vapors can rapidly initiate a local immune response. Recent evidence shows that exposure of immature dendritic cells from donors with rhinitis results in the production of IL-13 and maturation of a Th2 phenotype in autologous allergen-specific T cells (43). Interestingly, allergen exposure also up-regulated the production of IL-13 in immature dendritic cells isolated from nonallergic donors, supporting the hypothesis that Ag processing of allergenic molecules may induce a dendritic cell phenotype supportive of allergy development. Defining the cellular source of the IL-13 in the present model of TDI rhinitis may provide valuable insight into this hypothesis. The increased Th2 cytokine expression following challenge in naive mice corresponded with a small increase in eosinophil invasion. The relative increase in Th2 cytokine expression was lower in the sensitized mice than in the challenge-only mice despite the much greater eosinophil infiltration observed in sensitized mice. Greater relative expression of Th2 cytokines was also observed in the challenged group compared with the sensitized group, again with lower eosinophil counts in the challenged vs sensitized mice. These observations most likely reflect the temporal nature of the developing immune response, with Ag exposure inducing rapid increases in cytokine expression that results in a milieu conducive to inflammatory cell infiltration, a process that takes longer to develop.

The pathology and cytokine changes that characterize our model of TDI rhinitis were observed mainly in the anterior aspect of the nose. Inflammation was observed in the nasoturbinates, maxilloturbinates, and lateral wall of the nasal cavity, whereas negligible inflammation or remodeling occurred in the ethmoturbinates in the posterior region of the nose. Alterations in cytokine expression followed the same trend, with the highest expression levels observed in the anterior turbinates and lateral wall. These anatomic features are covered with transitional and respiratory epithelium, whereas the posterior ethmoturbinates are lined by olfactory epithelium (23). The distinct pattern of the allergic response observed in the present study may result from selective epithelial cell type sensitivity and/or regional dosimetry driven by reactivity, water solubility, and airflow (23). In the case of TDI, the latter is more likely because its chemical properties are a major determining factor. Monomeric TDI is a highly reactive bifunctional molecule that can bind with high affinity to many functional groups, particularly free amine groups on proteins (44, 45). This high reactivity suggests that TDI vapor will rapidly complex with epithelial and mucus proteins, effectively scrubbing it from the incoming air stream and reducing the concentration before reaching the olfactory epithelium in the posterior nasal cavity or the lung. Inhalation exposure paradigms at higher TDI concentrations or longer exposure durations induced lung pathology (10, 21, 24). This suggests that regional dose is most likely responsible for the pattern of response that will result from TDI vapor exposure, although it is still possible that selective sensitivity of transitional and respiratory epithelial cells vs olfactory epithelial cells plays a role. Future studies to define this relationship will be important for understanding the link between diisocyanate rhinitis and asthma.

Occupational rhinitis is a highly prevalent disease and is a comorbid condition in up to 92% of occupational asthma patients (4). The appearance of rhinitis symptoms in advance of asthma provides opportunities for early intervention and prevention (46). Realization of these opportunities necessitates a comprehensive understanding of the etiology and pathogenesis of occupational rhinitis. In summary, we have developed a novel murine model of TDI allergic rhinitis following inhalation exposure. Mice exposed to relatively low doses of TDI vapor displayed alterations in breathing pattern that corresponded with extensive eosinophilic inflammation and strong induction of immune/inflammatory cytokines and adhesion molecules. Systemic production of TDI-specific IgG Abs and increased total serum IgE were suggestive of immunologic sensitization. This model shows many of the characteristic features of allergic rhinitis in humans. As such, it may be useful in addressing pressing issues, including dosimetry/susceptibility, mechanisms of low m.w. chemical-induced rhinitis, and the relationship between upper and lower airways in respiratory allergy induced by diisocyanate exposure in the workforce.

Acknowledgments

We appreciate the support for the inhalation exposures, which were conducted by Amy Frazer, Michelle Donlin, and Jared Cumpston of the National Institute for Occupational Safety and Health Inhalation Facility (Morgantown, WV). The engineering support provided by Sam Stone (National Institute for Occupational Safety and Health) for chamber design is appreciated. We thank Dr. Lyndell Millecchia and Dean Newcomer (National Institute for Occupational Safety and Health) for their expert assistance with pathology preparation and imaging. We also thank Walter McKinney (National Institute for Occupational Safety and Health) for compiling the software application for automated analysis of Ab titers. We appreciate the excellent manuscript reviews by Drs. Paul Siegel,

Patti Zeidler-Erdely, and Paul Nicolaysen (National Institute for Occupational Safety and Health).

Disclosures

The authors have no financial conflict of interest.

References

1. Siracusa, A., M. Desrosiers, and A. Marabini. 2000. Epidemiology of occupational rhinitis: prevalence, aetiology and determinants. *Clin. Exp. Allergy* 30: 1519–1534.
2. Walusiak, J. 2006. Occupational upper airway disease. *Curr. Opin. Allergy Clin. Immunol.* 6: 1–6.
3. Gautrin, D., M. Desrosiers, and R. Castano. 2006. Occupational rhinitis. *Curr. Opin. Allergy Clin. Immunol.* 6: 77–84.
4. Malo, J. L., C. Lemiere, A. Desjardins, and A. Cartier. 1997. Prevalence and intensity of rhinoconjunctivitis in subjects with occupational asthma. *Eur. Respir. J.* 10: 1513–1515.
5. Lamb, C. E., P. H. Ratner, C. E. Johnson, A. J. Ambegaonkar, A. V. Joshi, D. Day, N. Sampson, and B. Eng. 2006. Economic impact of workplace productivity losses due to allergic rhinitis compared with select medical conditions in the United States from an employer perspective. *Curr. Med. Res. Opin.* 22: 1203–1210.
6. Johnson, V. J., and M. I. Luster. 2006. Animal models of occupational asthma: tools for understanding disease pathogenesis. In *Asthma in the Workplace and Related Conditions*, 3rd Ed. I. L. Bernstein, M. Chan-Yeung, J. L. Malo, and D. I. Bernstein, eds. Taylor and Francis, New York, pp. 141–160.
7. Redlich, C. A., and M. H. Karol. 2002. Diisocyanate asthma: clinical aspects and immunopathogenesis. *Int. Immunopharmacol.* 2: 213–224.
8. Maestrelli, P., A. di Stefano, P. Occari, G. Turato, G. Milani, F. Pivirotto, C. E. Mapp, L. M. Fabbri, and M. Saetta. 1995. Cytokines in the airway mucosa of subjects with asthma induced by toluene diisocyanate. *Am. J. Respir. Crit. Care Med.* 151: 607–612.
9. Maestrelli, P., P. Occari, G. Turato, S. A. Papiris, A. Di Stefano, C. E. Mapp, G. F. Milani, L. M. Fabbri, and M. Saetta. 1997. Expression of interleukin (IL)-4 and IL-5 proteins in asthma induced by toluene diisocyanate (TDI). *Clin. Exp. Allergy* 27: 1292–1298.
10. Matheson, J. M., V. J. Johnson, and M. I. Luster. 2005. Immune mediators in a murine model for occupational asthma: studies with toluene diisocyanate. *Toxicol. Sci.* 84: 99–109.
11. Herrick, C. A., L. Xu, A. V. Wisnewski, J. Das, C. A. Redlich, and K. Bottomly. 2002. A novel mouse model of diisocyanate-induced asthma showing allergic-type inflammation in the lung after inhaled antigen challenge. *J. Allergy Clin. Immunol.* 109: 873–878.
12. Meltzer, E. O. 2005. The relationships of rhinitis and asthma. *Allergy Asthma Proc.* 26: 336–340.
13. Jani, A. L., and D. L. Hamilos. 2005. Current thinking on the relationship between rhinosinusitis and asthma. *J. Asthma* 42: 1–7.
14. Littorin, M., L. Rylander, G. Skarping, M. Dalene, H. Welinder, U. Stromberg, and S. Skerfving. 2000. Exposure biomarkers and risk from gluing and heating of polyurethane: a cross sectional study of respiratory symptoms. *Occup. Environ. Med.* 57: 396–405.
15. Littorin, M., H. Welinder, G. Skarping, M. Dalene, and S. Skerfving. 2002. Exposure and nasal inflammation in workers heating polyurethane. *Int. Arch. Occup. Environ. Health* 75: 468–474.
16. Paggiaro, P. L., O. Rossi, L. Lastrucci, F. Pardi, A. Pezzini, and L. Baschieri. 1985. TDI-induced oculorhinitis and bronchial asthma. *J. Occup. Med.* 27: 51–52.
17. Baur, X., W. Marek, J. Ammon, A. B. Czuppon, B. Marczynski, M. Raulf-Heimsoth, H. Roemmelt, and G. Fruhmann. 1994. Respiratory and other hazards of isocyanates. *Int. Arch. Occup. Environ. Health* 66: 141–152.
18. Lemiere, C., P. Romeo, S. Chaboillez, C. Tremblay, and J. L. Malo. 2002. Airway inflammation and functional changes after exposure to different concentrations of isocyanates. *J. Allergy Clin. Immunol.* 110: 641–646.
19. Petsonk, E. L., M. L. Wang, D. M. Lewis, P. D. Siegel, and B. J. Husberg. 2000. Asthma-like symptoms in wood product plant workers exposed to methylene diphenyl diisocyanate. *Chest* 118: 1183–1193.
20. Matheson, J. M., V. J. Johnson, V. Vallyathan, and M. I. Luster. 2005. Exposure and immunological determinants in a murine model for toluene diisocyanate (TDI) asthma. *Toxicol. Sci.* 84: 88–98.
21. Matheson, J. M., R. W. Lange, R. Lemus, M. H. Karol, and M. I. Luster. 2001. Importance of inflammatory and immune components in a mouse model of airway reactivity to toluene diisocyanate (TDI). *Clin. Exp. Allergy* 31: 1067–1076.
22. Rando, R. J., Y. Y. Hammad, and S. N. Chang. 1989. A diffusive sampler for personal monitoring of toluene diisocyanate (TDI) exposure. I. Design of the dosimeter. *Am. Ind. Hyg. Assoc. J.* 50: 1–7.
23. Harkema, J. R., S. A. Carey, and J. G. Wagner. 2006. The nose revisited: a brief review of the comparative structure, function, and toxicologic pathology of the nasal epithelium. *Toxicol. Pathol.* 34: 252–269.
24. Johnson, V. J., B. Yucesoy, and M. I. Luster. 2005. Prevention of IL-1 signaling attenuates airway hyperresponsiveness and inflammation in a murine model of toluene diisocyanate-induced asthma. *J. Allergy Clin. Immunol.* 116: 851–858.
25. Pfaffl, M. W. 2001. A new mathematical model for relative quantification in real-time RT-PCR. *Nucleic Acids Res.* 29: e45.
26. Steel, R. G. D., and J. H. Torrie. 1980. *Principles and Procedures of Statistics: A Biometrical Approach.* McGraw-Hill, New York.
27. Johnson, V. J., J. M. Matheson, and M. I. Luster. 2004. Animal models for diisocyanate asthma: answers for lingering questions. *Curr. Opin. Allergy Clin. Immunol.* 4: 105–110.
28. Durham, S. R., S. Ying, V. A. Varney, M. R. Jacobson, R. M. Sudderick, I. S. Mackay, A. B. Kay, and Q. A. Hamid. 1992. Cytokine messenger RNA expression for IL-3, IL-4, IL-5, and granulocyte/macrophage-colony-stimulating factor in the nasal mucosa after local allergen provocation: relationship to tissue eosinophilia. *J. Immunol.* 148: 2390–2394.
29. Ciprandi, G., G. L. Marseglia, C. Klersy, and M. A. Tosca. 2005. Relationships between allergic inflammation and nasal airflow in children with persistent allergic rhinitis due to mite sensitization. *Allergy* 60: 957–960.
30. Ciprandi, G., A. Vizzaccaro, I. Cirillo, M. Tosca, A. Massolo, and G. Passalacqua. 2005. Nasal eosinophils display the best correlation with symptoms, pulmonary function and inflammation in allergic rhinitis. *Int. Arch. Allergy Immunol.* 136: 266–272.
31. Miyahara, S., N. Miyahara, K. Takeda, A. Joetham, and E. W. Gelfand. 2005. Physiologic assessment of allergic rhinitis in mice: role of the high-affinity IgE receptor (FcεRI). *J. Allergy Clin. Immunol.* 116: 1020–1027.
32. Cieslewicz, G., A. Tomkinson, A. Adler, C. Duez, J. Schwarze, K. Takeda, K. A. Larson, J. J. Lee, C. G. Irvin, and E. W. Gelfand. 1999. The late, but not early, asthmatic response is dependent on IL-5 and correlates with eosinophil infiltration. *J. Clin. Invest.* 104: 301–308.
33. Hessel, E. M., A. J. Van Oosterhout, C. L. Hofstra, J. J. De Bie, J. Garssen, H. Van Loveren, A. K. Verheyen, H. F. Savelkoul, and F. P. Nijkamp. 1995. Bronchoconstriction and airway hyperresponsiveness after ovalbumin inhalation in sensitized mice. *Eur. J. Pharmacol.* 293: 401–412.
34. Bachert, C., M. Wagenmann, and U. Hauser. 1995. Proinflammatory cytokines: measurement in nasal secretion and induction of adhesion receptor expression. *Int. Arch. Allergy Immunol.* 107: 106–108.
35. Bachert, C., M. Wagenmann, and G. Holtappels. 1998. Cytokines and adhesion molecules in allergic rhinitis. *Am. J. Rhinol.* 12: 3–8.
36. Terada, N., T. Nomura, W. J. Kim, Y. Otsuka, R. Takahashi, H. Kishi, T. Yamashita, N. Sugawara, S. Fukuda, T. Ikeda-Ito, and A. Konno. 2001. Expression of C-C chemokine TARC in human nasal mucosa and its regulation by cytokines. *Clin. Exp. Allergy* 31: 1923–1931.
37. Altman, G. B., L. C. Altman, D. L. Luchtel, A. J. Jabbour, and C. Baker. 1997. Release of RANTES from nasal and bronchial epithelial cells. *Cell Biol. Toxicol.* 13: 205–213.
38. Pease, J. E., and T. J. Williams. 2006. Chemokines and their receptors in allergic disease. *J. Allergy Clin. Immunol.* 118: 305–318.
39. Zabeau, L., P. Gevaert, C. Bachert, and J. Tavernier. 2003. Interleukin-5, eosinophilic diseases and therapeutic intervention. *Curr. Drug Targets Inflamm. Allergy* 2: 319–328.
40. Randolph, D. A., R. Stephens, C. J. Carruthers, and D. D. Chaplin. 1999. Cooperation between Th1 and Th2 cells in a murine model of eosinophilic airway inflammation. *J. Clin. Invest.* 104: 1021–1029.
41. Maestrelli, P., G. F. Del Prete, M. De Carli, M. M. D'Elios, M. Saetta, A. Di Stefano, C. E. Mapp, S. Romagnani, and L. M. Fabbri. 1994. CD8 T-cell clones producing interleukin-5 and interferon-γ in bronchial mucosa of patients with asthma induced by toluene diisocyanate. *Scand. J. Work Environ. Health* 20: 376–381.
42. Wisnewski, A. V., C. A. Herrick, Q. Liu, L. Chen, K. Bottomly, and C. A. Redlich. 2003. Human γ/δ T-cell proliferation and IFN-γ production induced by hexamethylene diisocyanate. *J. Allergy Clin. Immunol.* 112: 538–546.
43. Bellinghausen, I., P. Brand, I. Bottcher, B. Klostermann, J. Knop, and J. Saloga. 2003. Production of interleukin-13 by human dendritic cells after stimulation with protein allergens is a key factor for induction of T helper 2 cytokines and is associated with activation of signal transducer and activator of transcription-6. *Immunology* 108: 167–176.
44. Brown, W. E. 1986. The chemistry and biochemistry of isocyanates: an overview. In *Current Topics in Pulmonary Pharmacology and Toxicology.* M. A. Hollinger, ed. Elsevier, New York, pp. 200–225.
45. Brown, W. E., and A. L. Burkert. 2002. Biomarkers of toluene diisocyanate exposure. *Appl. Occup. Environ. Hyg.* 17: 840–845.
46. Nicholson, P. J., P. Cullinan, A. J. Taylor, P. S. Burge, and C. Boyle. 2005. Evidence based guidelines for the prevention, identification, and management of occupational asthma. *Occup. Environ. Med.* 62: 290–299.